

This is a repository copy of A comparison of approaches to compute the crack opening/sliding within the phase-field method.

White Rose Research Online URL for this paper: https://eprints.whiterose.ac.uk/id/eprint/232831/

Version: Published Version

Article:

Chen, L., Li, B., Cui, G. et al. (1 more author) (2025) A comparison of approaches to compute the crack opening/sliding within the phase-field method. Theoretical and Applied Fracture Mechanics, 136. 104818. ISSN: 0167-8442

https://doi.org/10.1016/j.tafmec.2024.104818

Reuse

This article is distributed under the terms of the Creative Commons Attribution (CC BY) licence. This licence allows you to distribute, remix, tweak, and build upon the work, even commercially, as long as you credit the authors for the original work. More information and the full terms of the licence here: https://creativecommons.org/licenses/

Takedown

If you consider content in White Rose Research Online to be in breach of UK law, please notify us by emailing eprints@whiterose.ac.uk including the URL of the record and the reason for the withdrawal request.



FISEVIER

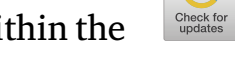
Contents lists available at ScienceDirect

Theoretical and Applied Fracture Mechanics

journal homepage: www.elsevier.com/locate/tafmec



A comparison of approaches to compute the crack opening/sliding within the phase-field method



L. Chen a,b, B. Li c, G. Cui a, R. de Borst d,*

- ^a Northeastern University, Key Laboratory of Ministry of Education on Safe Mining of Deep Metal Mines, Shenyang 110819, China
- ^b University of Dundee, School of Science and Engineering, Dundee DD1 4HN, UK
- ^c Guangdong Technion Israel Institute of Technology, Department of Mechanical Engineering, Shantou 515063, China
- ^d University of Sheffield, Department of Civil and Structural Engineering, Sheffield S1 3JD, UK

ARTICLE INFO

Keywords: Fracture Phase-field model Crack opening Crack sliding Mixed-mode Smeared crack model

ABSTRACT

The phase-field method has been used widely in the analysis of fracture due to its easy description of cracks, which obviates the introduction of geometric discontinuities in the domain. The discrete crack is regularised as a smeared surface, defined by a phase-field variable, and there is no need to explicitly define a crack path. Due to the smeared nature of the phase-field method, the crack opening and crack sliding do not directly result from a phase-field computation, but need to be computed a posteriori. Herein, we provide a complete overview of methods to compute the crack opening and crack sliding, resulting from the phase-field computation, namely the auxiliary field method, the integration method and the Taylor expansion method. The advantages and disadvantages of the methods are demonstrated by numerical examples, for crack opening/sliding. The auxiliary field and integration methods provide stable and relatively accurate results, but the Taylor expansion method is the faster approach to compute the crack opening/sliding, with a guaranteed accuracy.

1. Introduction

Phase-field modelling of cracks has gained popularity in the analysis of material failures over the past two decades, e.g., [1]. Developed initially for the analysis of brittle fracture, the method has now also been extended to cohesive fracture, e.g., [2]. In the phase-field method the discrete crack is regularised and represented as a smeared surface by a scalar variable (phase field). Due to the regularisation the intricate task of tracking a discrete crack surface, especially in 3D simulations, is avoided. Thus, the phase-field method allows to elegantly simulate complicated fracturing phenomena, including initiation, propagation, coalescence and branching.

The vast majority of phase-field analyses have been applied to brittle fracture, i.e. without surface tractions on the crack, e.g., [1,3,4]. Nevertheless, in many natural and human-induced fractures there are tractions on the crack surface, for instance in hydraulic fracturing and cohesive fracture. To include these tractions, one needs to know the crack opening, and in case of the mixed-mode fracturing, the crack sliding in order to compute the tractions applied on the crack surface.

For brittle fracture Chukwudozie et al. [5] proposed an integral approach to compute the crack opening in the normal direction, which they applied to the analysis of hydraulic fracture. The normal vector is defined by the phase-field gradient. Later, Lee et al. [6] and Yoshioka

et al. [7] used a level-set approach to obtain the crack normal vector, and this is applied in the integral of normal crack opening computation. The accuracy of this approach depends on the level set function. Recently, Chen et al. [8] extended this approach to include the shear direction for the brittle and cohesive fracture. Another approach to compute the crack opening in the normal direction is the integration of the functional of the degradation function and the homogeneous energy function [9-14]. Later, Feng et al. [15,16] extended this concept for the computation of crack sliding in the shear direction. They computed the cohesive strain in the regularised crack area, used as the integrand in the line integral. Fei et al. [17] employed the strain in the phase field regularised area to compute the crack opening in the normal direction. The force balance relation is considered in their analysis. The Dirac-delta function approximation from Chen et al. [18] is used in their formulation. Yin et al. [19] employed the representative crack element (RCE) concept to analyse the cohesive fracture problem. In their analysis the crack opening/sliding is obtained from the strain of the RCE element.

For cohesive fracture Verhoosel and de Borst [2] treated the cohesive interface in a smeared sense by the phase-field regularisation technique, and introduced an auxiliary field to model the crack opening/sliding, see also [20,21]. The auxiliary field is considered as an

E-mail address: r.deborst@sheffield.ac.uk (R. de Borst).

^{*} Corresponding author.

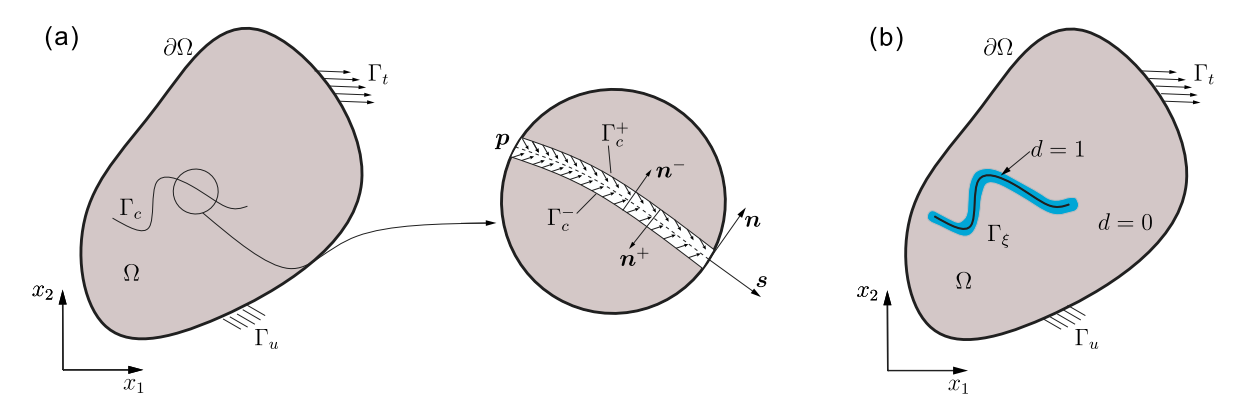


Fig. 1. Representation of a crack surface: (a) discrete form Γ_{ε} ; Γ_{c}^{+} and Γ_{c}^{-} are crack boundaries with positive and negative sides, respectively; (b) smeared form Γ_{ε} (blue area). Boundary Γ_{u} is prescribed with a displacement $\tilde{\mathbf{u}}$; Γ_{t} with a prescribed traction $\hat{\mathbf{t}}$.

independent variable in the simulation, similar to the displacement field. In their works, the exponential form of the phase field model (also known as AT2 model) has been considered. The support of the exponential function is spread over the entire domain. Recently, Chen and de Borst [22] introduced the sinusoidal form of the phase field model (known as PCM model) to regularised the crack surface, confining the smeared crack to a localised area. However, the auxiliary field approach requires the prescription of the auxiliary field (crack opening/sliding) degrees of freedom in the entire domain, similar to the displacement degrees of freedom.

Nguyen et al. [23] proposed a discrete-crack like approach to compute the crack opening/sliding. They applied the first order Taylor expansion to approximate the displacement and then computed the mixed-mode crack opening/sliding at two closed points along the crack. This is a direct approach, comparing to the integral approach and auxiliary approach. Obviously the solution of the crack opening/sliding relies on the choice of these points, and later an analytical expression was derived to compute the optimal location of these points [24]. Kumar et al. [25] and Paggi et al. [26] also suggested a direct concept to compute the crack opening/sliding. They employed the phase-field as the interpolation variable for the crack opening/sliding.

In this contribution, we will consider the integral approach of Chukwudozie et al. [5], further extended by Chen et al. [8], the auxiliary field approach and the Taylor expansion approach for the computation of the crack opening/sliding from the result of a phase-field analysis. The three approaches are concisely derived and discussed, and then compared in this contribution, including pros and cons. The study aims to provide a comprehensive illustration of the computation of the crack opening and crack sliding in the framework of phase-field modelling. The derivation of the formulations will be given.

We will start this contribution with a concise description of phasefield modelling. Subsequently, the ways to compute crack opening and crack sliding will be derived for the different approaches. An assessment is given in Section 4, where two examples are considered with complex crack patterns.

2. Phase-field model for fracture

In this section we will summarise the phase-field method for modelling fracture. Fig. 1 shows an open domain Ω with an internal discontinuity Γ_c with a possible traction p on this internal boundary.

2.1. Smeared crack representation

The key point of the phase-field method is the replacement of a discontinuity, denoted here as Γ_c , by a smeared surface Γ_ξ , as illustrated in Fig. 1(b). The width of Γ_ξ is governed by a regularisation parameter ℓ . An evolving phase field $d(\mathbf{x})$ is employed to describe Γ_ξ . $d(\mathbf{x}) = 1$

at the centre of Γ_c , and is vanishing away from Γ_c . The form of $d(\mathbf{x})$ is determined by a variational problem:

$$d(\mathbf{x}) = \operatorname{Arg} \left\{ \inf_{d \in S_d} \Gamma_d(d) \right\} \quad \text{with} \quad \Gamma_d(d) = \int_{\Omega} \gamma_d(d) \, dV \quad (1)$$

where $S_d = \left\{ d \mid d(\mathbf{x}) = 1 \ \forall \mathbf{x} \in \Gamma_c \right\}$. Γ_d denotes the total crack length per unit area. γ_d represents the crack density function per unit volume. In this study the following phase field function is employed [13]:

$$d\left(x_{n}\right) = \begin{cases} 1 - \sin\left(\frac{|x_{n}|}{\ell}\right) & -\pi\ell/2 \le x_{n} \le \pi\ell/2 \\ 0 & \text{otherwise} \end{cases}$$
 (2)

where $x_n = (\mathbf{x} - \mathbf{x}_c) \cdot n(\mathbf{x}_c)$, point \mathbf{x}_c on the discontinuity Γ_c and $n(\mathbf{x}_c)$ the unit vector normal to Γ_c . The corresponding Euler–Lagrange equation of this solution is given in [18], while the crack density function associated with Eq. (2) reads [13]:

$$\gamma_d(d) = \frac{1}{\pi \ell} \left(2d(\mathbf{x}) - d(\mathbf{x})^2 \right) + \frac{\ell}{\pi} \nabla d(\mathbf{x}) \cdot \nabla d(\mathbf{x})$$
 (3)

Chen et al. [22] have presented the profile of the phase field $d(x_n)$ and the crack density function $\gamma_d(d)$. From their analysis it appears that the distribution of $d(x_n)$ and $\gamma_d(d)$ is localised around the discontinuity Γ_c , thus confining the influence of the smeared form Γ_{ξ} , which is different from the classical phase field model (AT2 model). Moreover, the current phase field model guarantees the irreversibility condition in softening laws which are frequently adopted for quasibrittle failure [13]. This is a superior aspect of the current phase field model over the AT1 model.

2.2. Regularised fracture model

In this contribution we assume infinitesimal strains, linear elastic material behaviour and the absence of body forces. For the cracked body $\Omega \subseteq \mathbb{R}^n$ in Fig. 1, the variation of the energy functional reads:

$$\delta \mathcal{P}(\mathbf{u}, \Gamma; \mathbf{p}) = \int_{\Omega \setminus \Gamma} \delta \mathcal{W}(\mathbf{u}) \, \mathrm{d}\Omega - \int_{\Gamma_t} \delta \mathbf{u} \cdot \hat{\mathbf{t}} \, \mathrm{d}\Gamma - \int_{\Gamma_c} t_n \delta \left[\left[\mathbf{u} \cdot \mathbf{n} \right] \right] \, \mathrm{d}\Gamma$$
$$- \int_{\Gamma_c} t_s \delta \left[\left[\mathbf{u} \cdot \mathbf{s} \right] \right] \, \mathrm{d}\Gamma$$
(4)

with $\mathcal{W}(\mathbf{u})$ being the strain energy density function, $\mathcal{W}(\mathbf{u}) = \mu \, \boldsymbol{\varepsilon}(\mathbf{u}) \cdot \boldsymbol{\varepsilon}(\mathbf{u}) + \lambda/2 \mathrm{tr}(\boldsymbol{\varepsilon}(\mathbf{u}))^2$. λ and μ are the Lamé constants. $\boldsymbol{\varepsilon}(\mathbf{u}) = 1/2 \left(\nabla \mathbf{u} + \nabla \mathbf{u}^T \right)$ is the strain tensor. $\hat{\mathbf{t}}$ is the prescribed traction on the boundary Γ_t ; $p = \begin{bmatrix} t_n, t_s \end{bmatrix}$ is the prescribed traction on the discontinuity Γ_c . t_n is the normal traction exerted on Γ_c , while t_s is the shear traction along Γ_c . $[\![\mathbf{u} \cdot \boldsymbol{n}]\!]$ and $[\![\mathbf{u} \cdot \boldsymbol{s}]\!]$ are the crack opening/sliding at the discontinuity Γ_c in the normal and shear directions, respectively.

If the traction $p = [t_n, t_s]$ in Eq. (4) does not depend on the crack opening/sliding we can solve the problem in the framework of the brittle fracture model [18]. Else, for instance when the normal traction t_n is a pressure p exerted on a crack surface [5,7], or if the

shear traction t_s is a fluid shear stress [27], solving Eq. (4) becomes a challenging task. Phase-field modelling introduces a variational free-discontinuity formulation of brittle fracture, and considers the crack geometry and the displacement field simultaneously [1]. A Griffith-like energy functional is introduced to govern the crack initiation and evolution. A regularisation technique is proposed to smear the discontinuity [1]. In the regularised model, cracks are represented by the scalar phase field, $d(\mathbf{x})$. The form of $d(\mathbf{x})$ is given in Eq. (2). Then, the energy functional, Eq. (4), can be replaced by [1]:

$$\mathcal{P}(\mathbf{u}, \Gamma; \mathbf{p}) = \int_{\Omega} a(d) \, \mathcal{W}(\mathbf{u}) \, \mathrm{d}\Omega - \int_{\Gamma_t} \mathbf{u} \cdot \hat{\mathbf{t}} \, \mathrm{d}\Gamma - \int_{\Gamma_c} t_n \, [\![\mathbf{u} \cdot \mathbf{n}]\!] \, \mathrm{d}\Gamma$$
$$- \int_{\Gamma_c} t_s \, [\![\mathbf{u} \cdot \mathbf{s}]\!] \, \mathrm{d}\Gamma + \mathcal{G}_c \int_{\Omega} \gamma_d(d) \, \mathrm{d}\Omega$$
 (5)

where we do not provide the energy functional in the variational form for brevity sake. $a(d)=(1-d)^2$ is a degradation function. $\gamma_d(d)$ denotes the crack density function per unit volume, defined in Eq. (3). \mathcal{G}_c represents a scaling factor, with the dimension of energy per unit surface. The last term represents the fracture energy in the sense of Griffith's theory of brittle fracture [28]. Here, the terms, $\int_{\Gamma_c} t_n [\![\mathbf{u} \cdot \mathbf{n}]\!] \, \mathrm{d}\Gamma$ and $\int_{\Gamma_c} t_s [\![\mathbf{u} \cdot \mathbf{s}]\!] \, \mathrm{d}\Gamma$ are still provided in a discrete form, not regularised, due to unknown locations of the crack opening/sliding [5]. The smeared representations of $\int_{\Gamma_c} t_n [\![\mathbf{u} \cdot \mathbf{n}]\!] \, \mathrm{d}\Gamma$ and $\int_{\Gamma_c} t_s [\![\mathbf{u} \cdot \mathbf{s}]\!] \, \mathrm{d}\Gamma$ will be given in Section 3.2.

If the traction $p = [t_n, t_s]$ is a function of the crack opening/sliding we must solve the problem employing the cohesive fracture model [29]. Introduced in [30], the cohesive zone model is now widely used to model interface behaviour [29]. The essence of the model is a relation between the traction and the crack opening/sliding:

$$p = [t_n, t_s] = \mathbf{t}_d ([[\mathbf{u} \cdot \mathbf{n}]], [[\mathbf{u} \cdot \mathbf{s}]], \boldsymbol{\kappa})$$
(6)

with κ a history parameter, which obeys the Kuhn–Tucker conditions to distinguish between loading and unloading. \mathbf{t}_d , $[\![\mathbf{u}\cdot n]\!]$ and $[\![\mathbf{u}\cdot s]\!]$ are given in the local coordinate system (s,n), see Fig. 1. Different types of cohesive zone laws are available in the literature [31], such as the Xu–Needleman law, the bilinear law, etc. We can straightforwardly incorporate these cohesive zone laws.

Due to the dependence of the traction p on the crack opening/sliding, the energy functional, Eq. (4), in the cohesive zone model is reformulated as [29]:

$$\mathcal{P}(\mathbf{u}, \Gamma; \mathbf{p}) = \int_{\Omega} \mathcal{W}(\mathbf{u}) \, \mathrm{d}\Omega - \int_{\Gamma_{\mathbf{u}}} \mathbf{u} \cdot \hat{\mathbf{t}} \, \mathrm{d}\Gamma + \int_{\Gamma_{\mathbf{u}}} \mathcal{G}(\llbracket \mathbf{u} \cdot \mathbf{n} \rrbracket, \llbracket \mathbf{u} \cdot \mathbf{s} \rrbracket, \mathbf{\kappa}) \, \mathrm{d}A \tag{7}$$

 $G([[\mathbf{u} \cdot n]], [[\mathbf{u} \cdot s]], \kappa)$ is the fracture energy function, representing the energy dissipation upon the creation of a unit crack surface. It relies on the crack opening/sliding and is released gradually, linking to the traction p by a differential form:

$$t_{n} = \frac{\partial \mathcal{G}(\llbracket \mathbf{u} \cdot \mathbf{n} \rrbracket, \llbracket \mathbf{u} \cdot \mathbf{s} \rrbracket, \mathbf{\kappa})}{\partial \llbracket \mathbf{u} \cdot \mathbf{n} \rrbracket} \qquad t_{s} = \frac{\partial \mathcal{G}(\llbracket \mathbf{u} \cdot \mathbf{n} \rrbracket, \llbracket \mathbf{u} \cdot \mathbf{s} \rrbracket, \mathbf{\kappa})}{\partial \llbracket \mathbf{u} \cdot \mathbf{s} \rrbracket}$$
(8)

In the phase field framework the energy functional, Eq. (7), yields a phase-field regularised energy function for cohesive fracture [18]

$$\mathcal{E}(\mathbf{u}, \Gamma; \mathbf{p}) = \int_{\Omega} \mathcal{W}(\mathbf{u}) \, \mathrm{d}\Omega - \int_{\Gamma_{t}} \mathbf{u} \cdot \hat{\mathbf{t}} \, \mathrm{d}\Gamma$$

$$+ \int_{\Gamma} \mathcal{G}(\llbracket \mathbf{u} \cdot \mathbf{n} \rrbracket, \llbracket \mathbf{u} \cdot \mathbf{s} \rrbracket, \mathbf{\kappa}) \int_{x_{n} = -\infty}^{\infty} \delta(x_{n}) \, \mathrm{d}V$$

$$\approx \int_{\Omega} \mathcal{W}(\mathbf{u}) \, \mathrm{d}\Omega - \int_{\Gamma_{t}} \mathbf{u} \cdot \hat{\mathbf{t}} \, \mathrm{d}\Gamma$$

$$+ \int_{\Omega} \mathcal{G}(\llbracket \mathbf{u} \cdot \mathbf{n} \rrbracket, \llbracket \mathbf{u} \cdot \mathbf{s} \rrbracket, \mathbf{\kappa}) \, \delta_{c}(x_{n}) \, \mathrm{d}V$$

$$(9)$$

with \mathbf{x}_c being points on the fracture Γ_c ; $\mathbf{x}_n = (\mathbf{x} - \mathbf{x}_c) \cdot \mathbf{n} (\mathbf{x}_c)$ and $\mathbf{n} (\mathbf{x}_c)$ the unit vector normal to the crack Γ_c . $\delta_c (\mathbf{x}_n)$ is an approximation

of the Dirac-delta function $\delta(x_n)$, employed to express the infinitesimal area dA in an infinitesimal volume format dV, which takes the form [18]:

$$\delta_{c}(x_{n}) = \frac{1}{2} \left| \frac{\mathrm{d}d(x_{n})}{\mathrm{d}x_{n}} \right| = \frac{1}{2} \begin{cases} -\frac{\mathrm{d}d(x_{n})}{\mathrm{d}x_{n}} & 0 < x_{n} \leq \pi\ell/2 \\ \frac{\mathrm{d}d(x_{n})}{\mathrm{d}x_{n}} & -\pi\ell/2 \leq x_{n} \leq 0 \\ 0 & \text{otherwise} \end{cases}$$

$$= \frac{1}{2} \begin{cases} \frac{1}{\ell} \cos\left(\frac{x_{n}}{\ell}\right) & -\pi\ell/2 \leq x_{n} \leq \pi\ell/2 \\ 0 & \text{otherwise} \end{cases}$$

$$(10)$$

in which the fraction $\frac{1}{2}$ stems from the constraint on the Dirac-delta function, $\int_{-\infty}^{\infty} \delta_c(x_n) dx_n = 1$. Obviously $\delta_c(x_n)$ is localised around the crack Γ_c .

3. Computing the crack opening and sliding within the phase field method

The energy functional equations, (5) and (9), rely on the mixedmode crack opening/sliding, $[\![\mathbf{u} \cdot \mathbf{n}]\!]$ and $[\![\mathbf{u} \cdot \mathbf{s}]\!]$. However, the crack geometry Γ_c cannot be tracked explicitly in the phase-field model, and we cannot directly compute the mixed-mode crack opening/sliding in Eqs. (5) and (9). To compute $[\![\mathbf{u} \cdot \mathbf{n}]\!]$ and $[\![\mathbf{u} \cdot \mathbf{s}]\!]$. Verhoosel and de Borst [2] employed the phase-field regularisation to smear out the discrete cohesive fracture and simultaneously introduced an auxiliary field to model the mixed-mode crack opening/sliding. Nguyen et al. [23] adopted a similar regularisation strategy to represent the cohesive interface. However, to avoid the auxiliary field, they used a first-order Taylor expansion to compute the mixed-mode crack opening/sliding. Chen et al. [8] proposed an integral form to compute the mixed-mode crack opening/sliding in the framework of brittle and cohesive fracture. Until now, there is no comprehensive assessment of the various ways to compute the opening and sliding under mixed-mode conditions. In this section, we will summarise the various ways to compute the crack opening and crack sliding in a phase-field context.

The essence of the phase field model is to regularise the crack Γ_c by a smeared form Γ_{ξ} , as presented in Fig. 2(a). In the regularised framework, the normal vector \mathbf{n} can be approximated as [5]:

$$\boldsymbol{n} \approx -\nabla d\left(x_{n}^{+}\right) \mathbf{I} / \left|\nabla d\left(x_{n}^{+}\right)\right| = -\frac{1}{\left|\nabla d\left(x_{n}^{+}\right)\right|} \left[\frac{\partial d\left(x_{n}^{+}\right)}{\partial x_{1}} \frac{\partial d\left(x_{n}^{+}\right)}{\partial x_{2}}\right]$$

$$\approx \nabla d\left(x_{n}^{-}\right) \mathbf{I} / \left|\nabla d\left(x_{n}^{-}\right)\right|$$
(11)

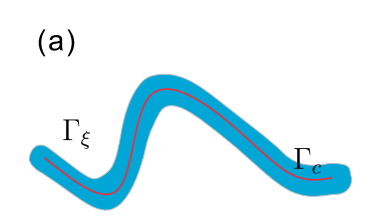
with $\left|\nabla d\left(x_{n}^{+}\right)\right| = \sqrt{\left(\frac{\partial d\left(x_{n}^{+}\right)}{\partial x_{1}}\right)^{2} + \left(\frac{\partial d\left(x_{n}^{+}\right)}{\partial x_{2}}\right)^{2}}$, and **I** a 2 × 2 identity matrix. The unit (shear) vector *s* along the crack Γ_{c} , see Fig. 1(a), can be obtained from the vector product of the normal vector *n* and the out-of-plane vector $z = [0 \ 0 \ 1]$:

$$s \approx \frac{1}{\left|\nabla d\left(x_{n}^{+}\right)\right|} \left[-\frac{\partial d\left(x_{n}^{+}\right)}{\partial x_{2}} \quad \frac{\partial d\left(x_{n}^{+}\right)}{\partial x_{1}}\right] = \frac{-\nabla d\left(x_{n}^{+}\right)\mathbf{I}_{a}}{\left|\nabla d\left(x_{n}^{+}\right)\right|}$$

$$\approx \frac{1}{\left|\nabla d\left(x_{n}^{-}\right)\right|} \left[\frac{\partial d\left(x_{n}^{-}\right)}{\partial x_{2}} \quad -\frac{\partial d\left(x_{n}^{-}\right)}{\partial x_{1}}\right] = \frac{\nabla d\left(x_{n}^{-}\right)\mathbf{I}_{a}}{\left|\nabla d\left(x_{n}^{-}\right)\right|}$$

$$(12)$$

with
$$\mathbf{I}_a = \begin{bmatrix} 1 & 0 \\ 0 & -1 \end{bmatrix}$$
.



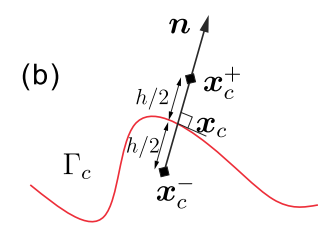


Fig. 2. (a) smeared representation, Γ_c , of a crack surface Γ_c ; (b) approximation of the crack opening/sliding across Γ_c . The crack surface Γ_c is introduced as the red line.

3.1. Auxiliary field based crack opening/sliding computation

In the cohesive-zone model, the crack opening/sliding is an essential input in the energy functional, see Eq. (9). In the phase-field modelling of cohesive fracture, Verhoosel and de Borst employed an auxiliary field, as an independent variable, to model the crack opening/sliding [2]. The model is a combination of discrete and smeared approaches. To describe the cohesive fracture behaviour, the cohesive-zone law from the discrete model is directly used. The phase-field regularisation is used to transfer the discrete interface into a smeared interface. Correspondingly, the crack opening/sliding [u] is regularised as:

$$\mathbf{[[u]]}(\mathbf{x}_{c}) = \underbrace{\int_{x_{n}=-\infty}^{\infty} \delta(x_{n}) dx_{n}}_{=1} \mathbf{[[u]]} = \int_{x_{n}=-\infty}^{\infty} \mathbf{v}(\mathbf{x}) \delta(x_{n}) dx_{n}$$

$$\approx \int_{x_{n}=-\infty}^{\infty} \mathbf{v}(\mathbf{x}) \delta_{c}(x_{n}) dx_{n}$$
(13)

with $\boldsymbol{v}(\boldsymbol{x})$ being an auxiliary field employed to approximate the crack opening/sliding in a smeared sense [22]; $\delta_c\left(x_n\right)$ is the approximated form of the Dirac-delta function $\delta\left(x_n\right)$, i.e. Eq. (10). $[\![\mathbf{u}]\!] = \mathbf{u}^+ - \mathbf{u}^- = \mathbf{R}^T \Big[\![\![\mathbf{u} \cdot \boldsymbol{s}]\!] \ [\![\![\mathbf{u} \cdot \boldsymbol{s}]\!]\!]^T$. \mathbf{u}^+ and \mathbf{u}^- being the displacement on the positive and negative sides, Γ_c^+ and Γ_c^- in Fig. 1(a), respectively. \mathbf{R} denotes a rotation matrix [29]. The divergence theorem is then applied to the weak form, Eq. (9), to obtain the elastic strain $\boldsymbol{\varepsilon}^e$ [2]:

$$\varepsilon_{ij}^{e} = u_{(i,j)} - \operatorname{sym}\left(v_{i}n_{j}\right)\delta_{c} \tag{14}$$

with $u_{(i,j)} = \frac{1}{2} \left(\frac{\partial u_i}{\partial x_j} + \frac{\partial u_j}{\partial x_i} \right)$ and n_j being the component of the unit vector normal to the interface Γ_c .

We next employ the variational principle for minimising $\mathcal{E}(\mathbf{u}, \Gamma; p)$ in Eq. (9) with respect to the displacement \mathbf{u} and the auxiliary field \mathbf{v} , which results in the weak form. Subsequently, we obtain the strong form of the displacement field \mathbf{u} and the auxiliary field \mathbf{v} in the framework of the phase-field method:

$$\begin{cases} \frac{\partial \sigma_{ij}}{\partial x_j} = 0 & x \in \Omega \\ \sigma_{ij} n_j = \hat{t}_i & x \in \Gamma_t \end{cases}$$
 (15a)

$$\begin{cases} \delta_{c} \left(t_{i}(\boldsymbol{v}, \boldsymbol{\kappa}) - \sigma_{ij} n_{j} \right) = \alpha \frac{\partial^{2} v_{i}}{\partial x_{n}^{2}} & \boldsymbol{x} \in \Gamma_{\xi} \\ \frac{\partial v_{i}}{\partial x_{n}} = 0 & \boldsymbol{x} \in \partial \Gamma_{\xi} \end{cases}$$
(15b)

with α being the penalty parameter, enforcing the constant crack opening/sliding condition in the crack normal direction n; σ_{ij} being the Cauchy stress and t_i being cohesive traction, defined as

$$\sigma_{ij} = \frac{\partial \mathcal{W}}{\partial \varepsilon_{ij}^e} \qquad \qquad t_i = \frac{\partial \mathcal{G}}{\partial v_i} \tag{16}$$

Eq. (15a) is standard in the continuum mechanics, while Eq. (15b) is an equilibrium equation over the smeared crack Γ_{ξ} . When $\ell \to 0$, the discrete cohesive traction is recovered from Eq. (15b): $t_i(\llbracket \mathbf{u} \rrbracket, \kappa) = \sigma_{ij} n_i$. The boundary condition in Eq. (15b) requires constant crack

opening/sliding at the boundary of the smeared crack, $\partial \Gamma_{\xi}$, necessitating fully prescribed auxiliary field (crack opening/sliding) degrees of freedom in the entire domain Ω [22]. In the simulation the finite element method can be used to solve Eq. (15) so as to obtain the displacement field \mathbf{u} and the auxiliary field (crack opening/sliding) \mathbf{v} [22].

3.2. Integration based crack opening/sliding computation

Chukwudozie et al. [5] proposed an integral form to compute the crack opening in the normal direction for the analysis of hydraulic fracturing in brittle porous media. Chen et al. [8] extended the integrating approach to the computation of the crack sliding. We will now describe the integral form of the mixed-mode crack opening/sliding for brittle and cohesive fracture.

3.2.1. Mixed-mode crack opening/sliding for brittle fracture

For the brittle fracture model, the crack opening in the normal direction can be expressed as:

$$\mathbf{[[}\mathbf{u}\cdot\boldsymbol{n}\mathbf{]]} = \mathbf{u}\left(x_{n}^{+}\right)\cdot\boldsymbol{n} - \mathbf{u}\left(x_{n}^{-}\right)\cdot\boldsymbol{n} \\
= \mathbf{u}\left(x_{n}^{+}\right)\cdot\boldsymbol{n}\int_{0}^{\infty}\left|\nabla d\left(x_{n}\right)\left|\mathrm{d}x_{n} - \mathbf{u}\left(x_{n}^{-}\right)\cdot\boldsymbol{n}\int_{-\infty}^{0}\left|\nabla d\left(x_{n}\right)\left|\mathrm{d}x_{n}\right|\right| \\
\approx \int_{0}^{\infty}\mathbf{u}\left(x_{n}\right)\cdot\boldsymbol{n}\left|\nabla d\left(x_{n}\right)\left|\mathrm{d}x_{n} - \int_{-\infty}^{0}\mathbf{u}\left(x_{n}\right)\cdot\boldsymbol{n}\left|\nabla d\left(x_{n}\right)\right|\mathrm{d}x_{n} \\
\approx -\int_{-\infty}^{\infty}\mathbf{u}\left(x_{n}\right)\cdot\left(\nabla d\left(x_{n}\right)\mathbf{I}\right)\mathrm{d}x_{n} = -\int_{-\pi\ell/2}^{\pi\ell/2}\mathbf{u}\left(x_{n}\right)\cdot\left(\nabla d\left(x_{n}\right)\mathbf{I}\right)\mathrm{d}x_{n}$$
(17)

with the normal vector \mathbf{n} in Eq. (11) and the identity relation $\int_{-\infty}^{0} \left| \nabla d \left(x_n \right) \right| \mathrm{d}x_n = \int_{0}^{\infty} \left| \nabla d \left(x_n \right) \right| \mathrm{d}x_n = 1$ being used. Similarly, the crack sliding in the shear direction can be obtained as:

$$\begin{aligned}
& [[\mathbf{u} \cdot s]] = \mathbf{u} (x_n^+) \cdot s - \mathbf{u} (x_n^-) \cdot s \\
& = \mathbf{u} (x_n^+) \cdot s \int_0^\infty \left| \nabla d (x_n) \right| dx_n - \mathbf{u} (x_n^-) \cdot s \int_{-\infty}^0 \left| \nabla d (x_n) \right| dx_n \\
& \approx \int_0^\infty \mathbf{u} (x_n) \cdot s \left| \nabla d (x_n) \right| dx_n - \int_{-\infty}^0 \mathbf{u} (x_n) \cdot s \left| \nabla d (x_n) \right| dx_n \\
& \approx - \int_{-\infty}^\infty \mathbf{u} (x_n) \cdot \left[\frac{\partial d (x_n)}{\partial x_2} - \frac{\partial d (x_n)}{\partial x_1} \right] dx_n \\
& = - \int_{-\pi\ell/2}^{\pi\ell/2} \mathbf{u} (x_n) \cdot \left(\nabla d (x_n) \mathbf{I}_a \right) dx_n
\end{aligned} \tag{18}$$

3.2.2. Mixed-mode crack opening/sliding for cohesive fracture

For cohesive fracture, the extended finite element approach (XFEM) can be used to derive the elastic strain Eq. (14), cf. [22] for details. Then, the displacement function can be expressed as the same form as in XFEM:

$$\mathbf{u}(\mathbf{x}) = \mathbf{w}(\mathbf{x}) + \mathcal{H}(\mathbf{x})\mathbf{v}(\mathbf{x}) \tag{19}$$

with w(x) being a continuous displacement function, and $\mathcal H$ being the Heaviside function, defined as [18]

$$\mathcal{H}(\mathbf{x}) = \frac{1}{2} \begin{cases} 1 & \pi\ell/2 \le x_n \\ \sin\left(\frac{x_n}{\ell}\right) & -\pi\ell/2 \le x_n \le \pi\ell/2 \\ -1 & \text{otherwise} \end{cases}$$
 (20)

For the cohesive fracture model the crack opening in the normal direction is obtained by multiplying Eq. (19) with the normal vector n, defined in Eq. (11), and integrating over the normal direction:

$$[\![\mathbf{u} \cdot \mathbf{n}]\!] = \mathbf{v}(\mathbf{x}) \cdot \mathbf{n} \approx -2 \int_{-\infty}^{\infty} \mathbf{u}(x_n) \cdot (\nabla d(x_n) \mathbf{I}) dx_n$$
 (21)

Similarly we obtain the crack sliding in the shear direction as:

$$[\![\mathbf{u} \cdot \mathbf{s}]\!] = \mathbf{v}(\mathbf{x}) \cdot \mathbf{s} \approx -2 \int_{-\infty}^{\infty} \mathbf{u}(x_n) \cdot (\nabla d(x_n) \mathbf{I}_a) dx_n$$
 (22)

Finally, the integral form of the mixed-mode crack opening/sliding can be summarised as:

$$\left[\left[\left[\mathbf{u} \cdot \mathbf{n} \right] \right] \left[\mathbf{u} \cdot \mathbf{s} \right] \right] \approx -1 \cdot k \cdot \int_{-\infty}^{\infty} \left[\mathbf{u} \left(x_n \right) \cdot \left(\nabla d \left(x_n \right) \mathbf{I} \right) \right] \mathbf{u} \left(x_n \right) \cdot \left(\nabla d \left(x_n \right) \mathbf{I}_a \right) \right] dx_n$$
(23)

with the coefficient k:

$$k = \begin{cases} 1 & \text{brittle fracture} \\ 2 & \text{cohesive fracture} \end{cases}$$
 (24)

3.3. Taylor expansion based crack opening/sliding computation

For phase-field modelling of cohesive fracture, Nguyen et al. [23] employed a first-order Taylor expansion to approximate the displacement field. They evaluated the crack opening/sliding at two points near the crack, similar to the discrete crack model [2]. However, the choice of the location of these points suffers from a certain arbitrariness.

It is possible to derive the optimal location of these points [24]. In phase-field modelling, the displacement field \mathbf{u} is continuous in the whole domain. We can therefore employ a first-order Taylor expansion of \mathbf{u} to approximate the displacement field around the crack Γ_c , see

$$\mathbf{u}\left(\mathbf{x}_{c}^{+}\right) = \mathbf{u}\left(\mathbf{x}_{c} + \frac{h}{2}\boldsymbol{n}\right) \approx \mathbf{u}\left(\mathbf{x}_{c}\right) + \frac{h}{2}\nabla\mathbf{u}\boldsymbol{n}$$

$$\mathbf{u}\left(\mathbf{x}_{c}^{-}\right) = \mathbf{u}\left(\mathbf{x}_{c} - \frac{h}{2}\boldsymbol{n}\right) \approx \mathbf{u}\left(\mathbf{x}_{c}\right) - \frac{h}{2}\nabla\mathbf{u}\boldsymbol{n}$$
(25)

with \mathbf{x}_c being a point on the crack Γ_c , n being the unit normal vector to the crack Γ_c , and h being a distance parameter. Then, the mixed-mode crack opening/sliding can be approximated as:

$$[[\mathbf{u}]](\mathbf{x}_c) \approx \mathbf{v}(\mathbf{x}_c) = \mathbf{u}\left(\mathbf{x}_c + \frac{h}{2}\mathbf{n}\right) - \mathbf{u}\left(\mathbf{x}_c - \frac{h}{2}\mathbf{n}\right) = h\nabla\mathbf{u}\mathbf{n}$$
 (26)

with $v(x_i)$ being the approximation of the crack opening/sliding. Subsequently, optimal location of these points can be derived analytically:

$$h = \frac{2\ell}{1 + 2k\ell/E} \tag{27}$$

with k being the cohesive fracture stiffness [24]; E being the Young's modulus. It normally holds that $k\ell \ll E$ [32]. Furthermore, to properly represent the fracture behaviour, the regularisation length ℓ should be small [2,22,23], which results in an approximated optimal distance parameter:

$$h = 2\ell \tag{28}$$

leading to the approximated form of the mixed-mode crack opening/sliding:

$$[\![\mathbf{u}]\!](\mathbf{x}_c) \approx \mathbf{v}(\mathbf{x}_c) \approx 2\ell \nabla \mathbf{u} \mathbf{n}$$
(29)

In general, these three crack opening/sliding computation approaches require the regularisation of the crack surface. The line

integration (2D case) or surface integration (3D case) of the fracture energy \mathcal{G} is transferred into a volume integration. The mixed-mode crack opening/sliding from the auxiliary field approach is obtained from the solution of the governing Eq. (15). It is obtained directly from the finite element solution of the weak form Eq. (9), similar to the computation of the phase-field variable in the brittle phase-field method [1]. The integration approach and Taylor expansion approach employ the solution of the displacement \mathbf{u} to compute the mixed-mode crack opening/sliding, i.e., a post-processing approach.

The Taylor expansion approach uses fewer degrees of freedom (u only) than the auxiliary field approach (both \mathbf{u} and \mathbf{v}). The integration approach utilises the same degrees of freedom as the Taylor expansion approach. However, it requires more computational effort to obtain the mixed-mode crack opening/sliding, due to the integration in Eq. (23). The crack opening/sliding in the auxiliary approach directly results from solving the governing equations, which is likely more accurate and reliable than results from post-processing. The integration approach averages the displacement field in the crack normal direction, avoiding numerically unstable displacement solutions. Thus, the crack opening/sliding solution of the auxiliary approach and integration approach should be more accurate than that of the Taylor expansion approach. In general, the Taylor expansion approach is the simpler and probably the faster approach to accurately obtain the crack opening and sliding. However, it is likely less accurate compared to the auxiliary and integration approaches. This will be validated by the numerical examples in Section 4.

4. Numerical comparisons

Two examples are now presented to compare the proposed formulations, analytically through an edge-cracked problem and numerically through curved crack scenario. First, we will consider a square plate (dimension 1×1) with an edge crack. In the analysis we consider Mode II-loading. For the analytical solution of the crack opening/sliding we refer to [33]. Next, an example is given of a curved, traction-free crack under uniaxial tension in order to demonstrate the performance of the methodology in a multi-dimensional setting. To well represent the crack in a smeared sense, the regularisation length is always chosen as $l \geq 4h$ (h: element size around the crack) [28]. We employ the integration approach of the brittle fracture model (Section 3.2.1), the auxiliary field approach (Section 3.3).

For the comparisons we have chosen the cases of cracks with a predefined path because of the availability of analytical solutions or reference solutions from other numerical approaches. We consider not only a linear crack, but also curved cracks. We have employed the phase field to define the crack paths. In the computation there are thus no geometric discontinuities.

4.1. Square plate under Mode II-loading

We consider en edge-cracked plate under Mode-II loading, shown in Fig. 3(a). The length of the initial crack is a=0.5. Plane-stress conditions are assumed. With a suitable re-scaling of the loading the material properties can be chosen as: Young's modulus E=1.0 and Poisson's ratio $\nu=0.3$. In Fig. 3(a), we consider the displacement on the boundary corresponding to the singular stress field (parameterised by the stress intensity factor $K_{\rm II}$) around the initial crack tip. The analytical expressions for the displacement field are given as:

$$u_{1} = \frac{K_{II}}{2\mu} \sqrt{\frac{r}{2\pi}} \sin \frac{\theta}{2} \left(2 + \kappa + \cos \theta \right)$$

$$u_{2} = \frac{K_{II}}{2\mu} \sqrt{\frac{r}{2\pi}} \cos \frac{\theta}{2} \left(2 - \kappa - \cos \theta \right)$$
(30)

with $K_{\rm II}=0.5$ in the current study. $\mu=E/2(1+\nu), \ \kappa=3-4\nu$ for plane strain and $\kappa=(3-\nu)/(1+\nu)$ for plane stress, and (r,θ) are polar

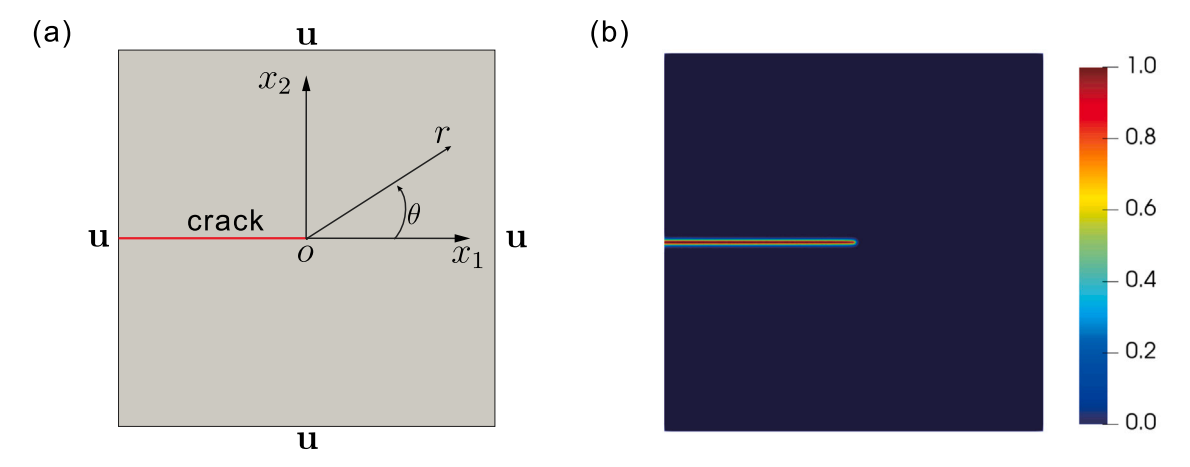


Fig. 3. (a) geometry of an edge-cracked square plate under Mode-II loading; (b) phase-field representation of the crack, the regularisation length is chosen as $\ell = 0.01$. In (a), the initial crack is introduced as the red line.

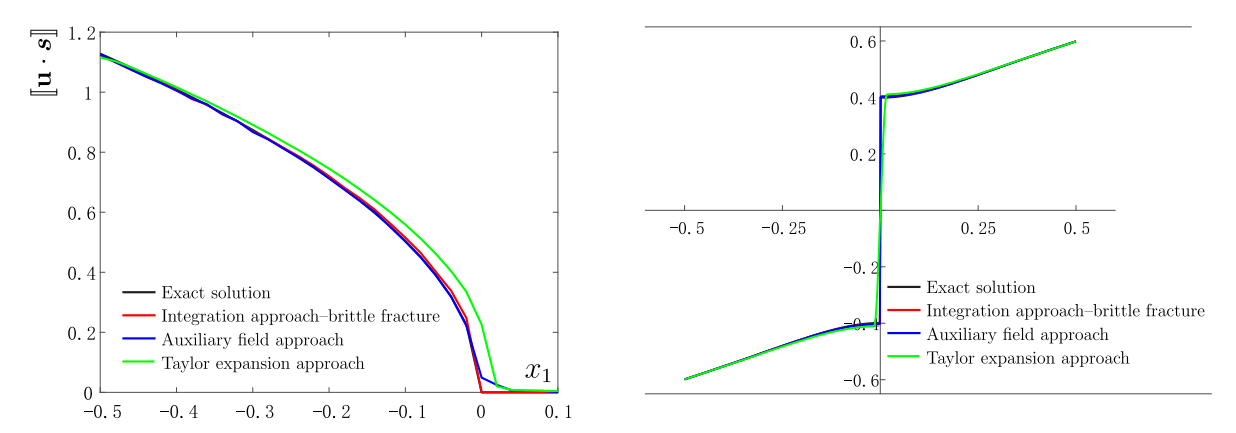


Fig. 4. Crack sliding in the shear direction $[u \cdot s]$ (left) and displacement $u_1(x_1 x_2)$ at $x_1 = -0.25$ (right) for Mode-II loading.

coordinates with the origin positioned at the crack tip, Fig. 3(a). The closed-form solution for the crack opening/sliding is given by:

$$\llbracket \mathbf{u} \rrbracket \left(\mathbf{x}_c \right) = \left\{ \llbracket \mathbf{u} \cdot \mathbf{n} \rrbracket \quad \llbracket \mathbf{u} \cdot \mathbf{s} \rrbracket \right\} = \left[0 \quad \frac{\mathbf{K}_{\Pi}}{\mu} \sqrt{\frac{r}{2\pi}} \left(\kappa + 1 \right) \right]$$
(31)

as we only have the crack sliding in the shear direction for Mode-II loading.

Fig. 3(b) shows the smeared crack, i.e. the coloured area, by the phase-field regularisation technique in Section 2.1. Fig. 4 shows the comparison between the numerical solutions and the analytical solutions. The results of numerical solutions agree well with analytical solutions, especially the displacement in Fig. 4(right). This validates the proposed formulations of the crack opening/sliding. The solution of Taylor expansion approach gives a slight difference in the plot of the shear crack sliding, see Fig. 4(left). The Taylor expansion approach relies on the choice of the distance parameter h in Eq. (26). Even we employ the optimal h in Eq. (28) to compute the mixed-mode crack opening/sliding, the formulation is still an approximation of the crack opening/sliding due to the first-order Taylor expansion. The influence of the higher-order term in the Taylor expansion is ignored, inducing the approximation error in the shear crack sliding $[u \cdot s]$.

The contour plot of the displacement field is shown in Fig. 5. In the figure, the displacement is discontinuous along the crack Γ_c in the integration approach, due to the brittle fracture model, while it is continuous in the auxiliary field approach and Taylor expansion approach, due to the continuous Dirac-delta function definition in Eq. (10). This can also be seen in Fig. 4.

4.2. Curved crack under uniaxial tension

We next consider a curved crack under uniaxial loadings. The set-up of the problem is shown in Fig. 6(a). The curved crack is prescribed in the left bottom of the plate, starting at (5, 0) and ending at $(5\cos\theta, 5\sin\theta)$. The arc angle is set as $\theta=45^\circ$. Plane-stress conditions are again adopted. With a suitable re-scaling, the material properties can be chosen as: Young's modulus E=1.0 and Poisson's ratio v=0.3. The curved crack is regularised as a smeared surface, presented in Fig. 6(b). No analytical solutions are available for this problem, only the discrete interface solution taken as the reference solution [29].

Fig. 7(a) presents the comparison of the mixed-mode crack opening/sliding between the proposed approaches in Section 3 and the discrete interface solution. Clearly, the results of the proposed approaches match well with those of the discrete interface model, again validating the formulation of the mixed-mode crack opening/sliding computation. The profile of the displacement ${\bf u}$ is shown in Fig. 8. The solutions of the proposed approaches agree well with each other. We observe slight difference of the displacement ${\bf u}$ along the crack Γ_c . A continuous displacement field is obtained across Γ_c for the auxiliary field approach and the Taylor expansion approach, while it is discontinuous for the integration approach due to the use of the brittle fracture model, as also shown in Fig. 7(b).

5. Concluding remarks

Phase-field models employ regularisation to transform a discrete crack into an equivalent smeared crack. For brittle fracture the crack

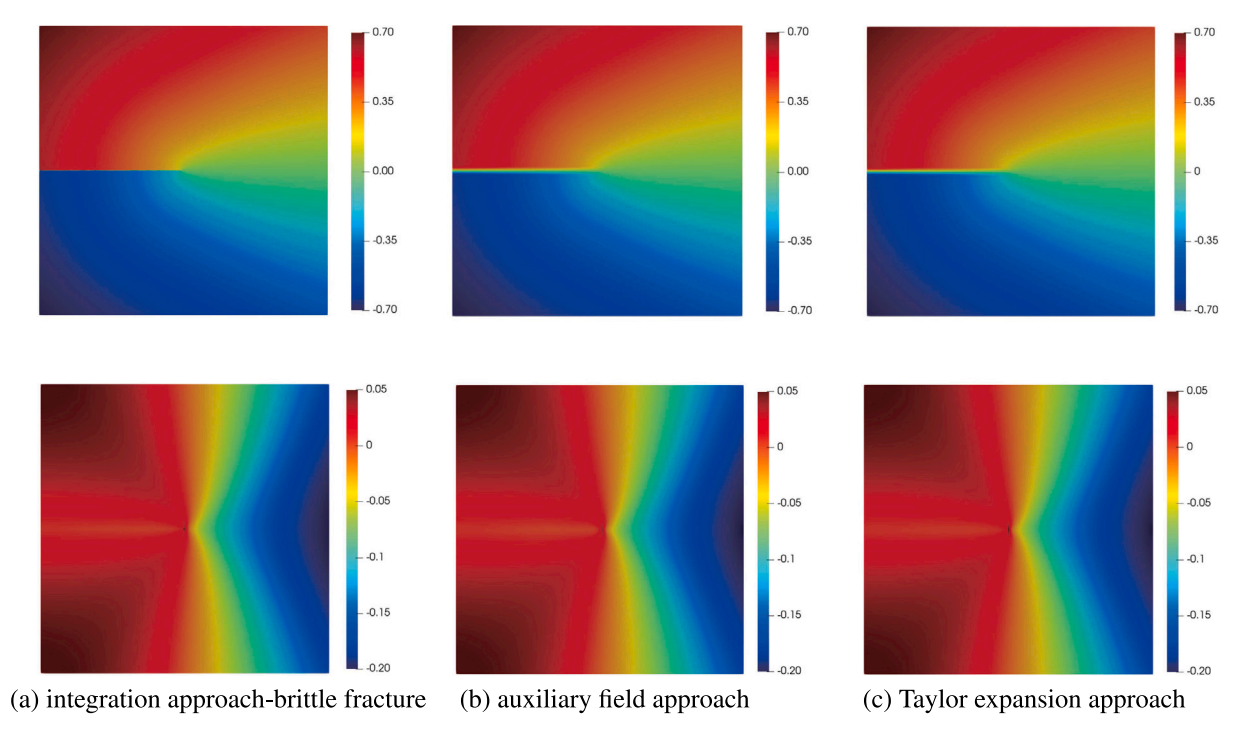


Fig. 5. Contour plot of displacement u_1 (upper row) and u_2 (bottom row) for Mode-II loading.

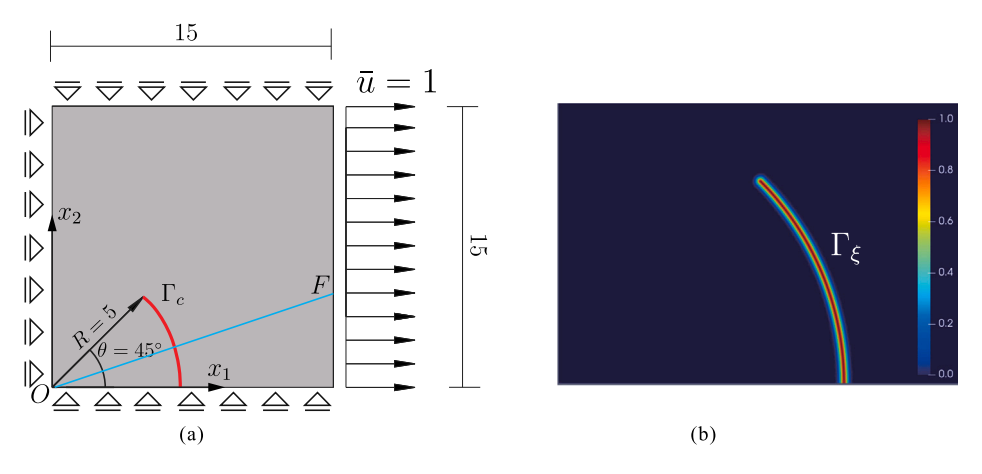


Fig. 6. (a) setup of a curved crack problem, the initial crack Γ_{ε} is introduced as the red line; (b) smeared crack Γ_{ξ} . The regularisation length is chosen as $\ell=0.1$. Figure (b) shows the left bottom part of the plate.

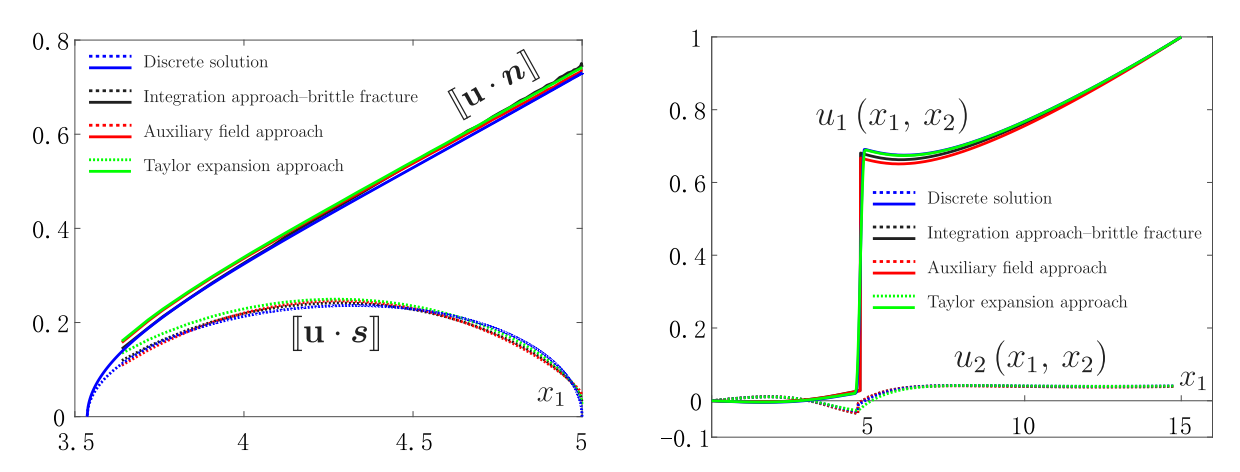


Fig. 7. (a) crack opening in the normal direction $[\![\mathbf{u}\cdot\mathbf{n}]\!]$ and in the shear direction $[\![\mathbf{u}\cdot\mathbf{s}]\!]$; (b) displacement $u_1\left(x_1,x_2\right)$ and $u_2\left(x_1,x_2\right)$ along the blue line *OF* in Fig. 6(a). Point *F* is with the coordinate $(x_1,x_2)=(15,5)$.

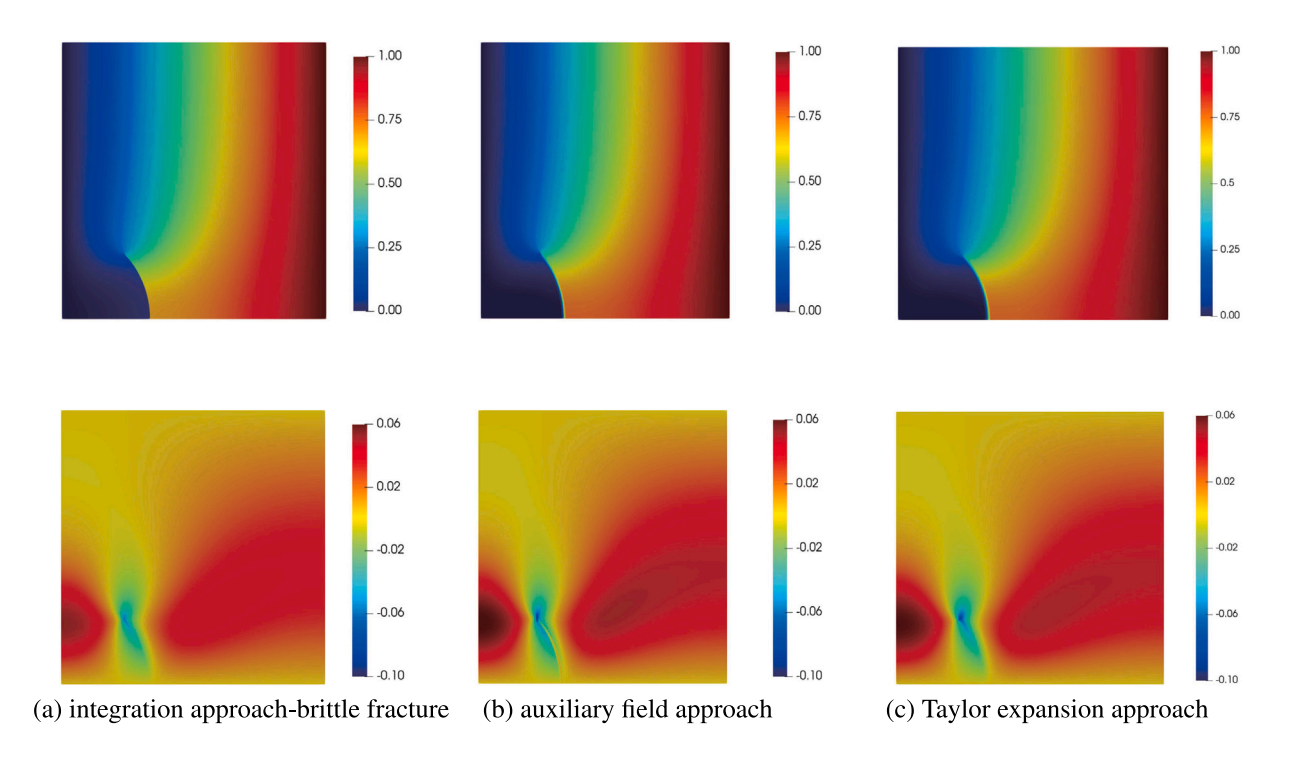


Fig. 8. Contour plot of displacement u_1 (upper row) and u_2 (bottom row) for the curved crack problem.

trajectory is obtained from the solution of the governing equation of the phase-field variable. For cohesive fracture the phase-field variable is used to regularise the crack opening/sliding dependent fracture energy. In certain applications the crack opening/sliding is an essential variable in the analysis, e.g., in hydraulic fracturing, or fibre-matrix debonding. However, the computation of the crack opening/sliding is not straightforward in a phase-field framework due to unknown crack trajectories.

In the simulation we need to employ some special strategies to approximate the crack opening/sliding. The crack opening/sliding can be introduced as an independent variable (auxiliary field) and computed by the solution of governing equations, already implemented in the cohesive fracture model. Due to the phase-field regularisation of the crack path the crack normal and shear vectors can then be computed by the phase-field gradient. The crack opening/sliding can also be obtained by the integration of the product of the displacement and the phase-field gradient. And even if no geometric discontinuities are introduced in the phase-field model, the crack opening/sliding can also be computed from two neighbouring points along the crack path (Taylor expansion form). The optimal distance is available for the choice of these two points.

From the numerical analysis these three approaches of the crack opening/sliding computation lead to similar results, validating the approaches. Generally, the auxiliary field approach gives a stable and accurate solution, but imposes a strong computation burden, due to the introduction of additional crack opening/sliding variable (auxiliary field). The integration approach also yields a stable and accurate solution, considering the averaging form of the integral. However, carrying out the integration reduces the efficiency. The Taylor expansion approach is the fastest method to compute the mixed-mode crack opening/sliding, only involving simple arithmetic calculations along the crack. However it can be less accurate than the other two approaches.

CRediT authorship contribution statement

L. Chen: Writing – original draft, Supervision, Software, Formal analysis, Conceptualization. **B. Li:** Software, Formal analysis, Conceptualization. **G. Cui:** Software, Formal analysis. **R. de Borst:** Writing – review & editing, Supervision, Conceptualization.

Declaration of competing interest

The authors declare that they have no known competing financial interests or personal relationships that could have appeared to influence the work reported in this paper.

Acknowledgements

The second author Bin Li was supported by the Guangdong Basic and Applied Basic Research Foundation, China under Grant No. 2024A1515011784.

Data availability

No data was used for the research described in the article.

References

- B. Bourdin, G.A. Francfort, J.J. Marigo, Numerical experiments in revisited brittle fracture, J. Mech. Phys. Solids 48 (2000) 797–826.
- [2] C.V. Verhoosel, R. de Borst, A phase-field model for cohesive fracture, Internat. J. Numer. Methods Engrg. 96 (2013) 43–62.
- [3] M.J. Borden, C.V. Verhoosel, M.A. Scott, T.J.R. Hughes, C.M. Landis, A phase-field description of dynamic brittle fracture, Comput. Methods Appl. Mech. Engrg. 217–220 (2012) 77–95.

- [4] J.-F. Shao, Z. Yu, Z. Liu, M.-N. Vu, G. Armand, Numerical analysis of thermohydromechanical process related to deep geological radioactive repository, Deep Resour. Eng 1 (1) (2024) 100001.
- [5] C. Chukwudozie, B. Bourdin, K. Yoshioka, A variational phase-field model for hydraulic fracturing in porous media, Comput. Methods Appl. Mech. Engrg. 347 (2019) 957–982.
- [6] S. Lee, M.F. Wheeler, T. Wick, Iterative coupling of flow, geomechanics and adaptive phase-field fracture including level-set crack width approaches, J. Comput. Appl. Math. 314 (2017) 40–60.
- [7] K. Yoshioka, D. Naumov, O. Kolditz, On crack opening computation in variational phase-field models for fracture, Comput. Methods Appl. Mech. Engrg. 369 (2020) 113210.
- [8] L. Chen, B. Li, R. de Borst, Integral form of mixed-mode crack opening in the phase field method, Theor. Appl. Fract. Mech. (2024) 104481.
- [9] K. Pham, J.-J. Marigo, C. Maurini, The issues of the uniqueness and the stability of the homogeneous response in uniaxial tests with gradient damage models, J. Mech. Phys. Solids 59 (6) (2011) 1163–1190.
- [10] K. Pham, J.-J. Marigo, From the onset of damage to rupture: construction of responses with damage localization for a general class of gradient damage models, Contin. Mech. Thermodyn. 25 (2013) 147–171.
- [11] E. Lorentz, S. Cuvilliez, K. Kazymyrenko, Modelling large crack propagation: from gradient damage to cohesive zone models. Int. J. Fract. 178 (2012) 85–95.
- [12] S. Conti, M. Focardi, F. Iurlano, Phase field approximation of cohesive fracture models, Ann. l'Institut Henri Poincaré C, Analyse non linéaire 33 (2016) 1033–1067.
- [13] J.Y. Wu, A unified phase-field theory for the mechanics of damage and quasi-brittle failure, J. Mech. Phys. Solids 103 (2017) 72–99.
- [14] F. Freddi, F. Iurlano, Numerical insight of a variational smeared approach to cohesive fracture, J. Mech. Phys. Solids 98 (2017) 156–171.
- [15] Y. Feng, J. Fan, J. Li, Endowing explicit cohesive laws to the phase-field fracture theory, J. Mech. Phys. Solids 152 (2021) 104464.
- [16] Y. Feng, J. Li, A unified regularized variational cohesive fracture theory with directional energy decomposition, Internat. J. Engrg. Sci. 182 (2023) 103773.
- [17] F. Fei, J. Choo, Crack opening calculation in phase-field modeling of fluid-filled fracture: A robust and efficient strain-based method, Comput. Geotech. 177 (2025) 106890.
- [18] L. Chen, R. de Borst, Computation of the crack opening displacement in the phase-field model, Int. J. Solids Struct. (2023).

- [19] B. Yin, D. Zhao, J. Storm, M. Kaliske, Phase-field fracture incorporating cohesive adhesion failure mechanisms within the representative crack element framework, Comput. Methods Appl. Mech. Engrg. 392 (2022) 114664.
- [20] S. May, J. Vignollet, R. de Borst, A numerical assessment of phase-field models for brittle and cohesive fracture: Γ-convergence and stress oscillations, Eur. J. Mech. A Solids 52 (2015) 72–84.
- [21] Y. Ghaffari Motlagh, R. de Borst, Considerations on a phase-field model for adhesive fracture, Internat. J. Numer. Methods Engrg. 121 (2020) 2946–2963.
- [22] L. Chen, R. de Borst, Phase-field regularised cohesive zone model for interface modelling, Theor. Appl. Fract. Mech. 122 (2022) 103630.
- [23] T.-T. Nguyen, J. Yvonnet, Q.-Z. Zhu, M. Bornert, C. Chateau, A phase-field method for computational modeling of interfacial damage interacting with crack propagation in realistic microstructures obtained by microtomography, Comput. Methods Appl. Mech. Engrg. 312 (2016) 567–595.
- [24] R. de Borst, L. Chen, Phase-field modelling of cohesive interface failure, Internat. J. Numer. Methods Engrg. (2023).
- [25] P.A.V. Kumar, A. Dean, J. Reinoso, M. Paggi, A multi phase-field-cohesive zone model for laminated composites: Application to delamination migration, Compos. Struct. 276 (2021) 114471.
- [26] M. Paggi, M. Corrado, J. Reinoso, Fracture of solar-grade anisotropic polycrystalline silicon: A combined phase field-cohesive zone model approach, Comput. Methods Appl. Mech. Engrg. 330 (2018) 123–148.
- [27] B. Werner, V. Myrseth, A. Saasen, Viscoelastic properties of drilling fluids and their influence on cuttings transport, J. Pet. Sci. Eng. 156 (2017) 845–851.
- [28] B. Bourdin, G.A. Francfort, J.J. Marigo, The variational approach to fracture, J. Elasticity 91 (2008) 5–148.
- [29] L. Chen, R. de Borst, Cohesive fracture analysis using Powell-Sabin B-splines, Int. J. Numer. Anal. Methods Geomech. 43 (2019) 625–640.
- [30] D.S. Dugdale, Yielding of steel sheets containing slits, J. Mech. Phys. Solids 8 (1960) 100–104.
- [31] K. Park, G.H. Paulino, Cohesive zone models: a critical review of tractionseparation relationships across fracture surfaces, Appl. Mech. Rev. 64 (2011) 060802
- [32] L. Chen, F.J. Lingen, R. de Borst, Adaptive hierarchical refinement of NURBS in cohesive fracture analysis, Internat. J. Numer. Methods Engrg. 112 (2017) 2151–2173
- [33] L. Chen, H. Bahai, G. Alfano, Extended Powell–Sabin finite element scheme for linear elastic fracture mechanics, Eng. Fract. Mech. 274 (2022) 108719.